Supplemental Material for

THREE DISTINCT MODES OF EXOCYTOSIS REVEALED BY AMPEROMETRY IN NEUROENDOCRINE CELLS

G.Th.H. van Kempen[1], H.T. vanderLeest[1], R.J. van den Berg[1], P. Eilers[2] and R.H.S. Westerink[3 *]

[1] Department of Molecular Cell Biology, Leiden University Medical Center, Leiden, The Netherlands.
[2] Department of Biostatistics, Erasmus University, Rotterdam, The Netherlands.
[3] Neurotoxicology Research Group, Toxicology Division, Institute for Risk Assessment Sciences (IRAS), Utrecht University, Utrecht, The Netherlands.

[*] Corresponding author: R.H.S. Westerink, Neurotoxicology Research Group, Toxicology Division, Institute for Risk Assessment Sciences (IRAS), Utrecht University, PO Box 80.177, 3508 TD Utrecht, The Netherlands.
E-mail: r.westerink@uu.nl

Supplementary Material and Methods

Carbon fiber amperometry

Carbon fiber electrodes (5 μm fiber diameter ProCFE, Dagan Corporation, Minneapolis, USA) were treated with Sylgard (Dow Corning, Midland, USA) to reduce noise (rms ± 1 pA, 30–5 kHz bandwidth) and were rinsed with ethanol between experiments. Amplifiers (axopatch-200A: Axon Instruments, Molecular Devices Corporation, Union City, USA; and EPC7: List Electronic, Darmstadt, Germany) were set at a cut-off frequency of 10 kHz (4-pole low-pass Bessel) and the amperometric current was sampled at a frequency of 20 kHz. The carbon fiber tip, polarized to +800 mV, was gently pressed on the surface of a single neuroendocrine cell with a bright halo-appearance. Cells that displayed an outburst of exocytotic spikes after placing the electrode or a fading bright halo-appearance were excluded to ensure measurements from undamaged and healthy cells only. Cells were continuously superfused with saline solution containing (in mM): 125 NaCl, 5.5 KCl, 2 $CaCl_2$, 0.8 $MgCl_2$, 10 HEPES, 24 glucose, 36.5 sucrose, pH adjusted to 7.3. Exocytosis was evoked by depolarizing PC12 and chromaffin cells by superfusion with a saline solution containing 60 mM or 125 mM KCl, respectively (NaCl was reduced to maintain isotonicity at ± 310 mOsM). Only one recording per culture dish was made to avoid effects of a previous KCl-depolarization. All experiments were performed at 20-22°C.

Event detection and selection

Amperometry allows for detection of exocytosis with high temporal resolution and accuracy only if release sites are under or very close to the sensitive surface of the carbon fiber ("near" sites). CA released at "far" sites will diffuse away and will not reach the detector at all, whereas molecules released at the "surround" sites (Fig. S1A) are detected with diffusional delays and attenuated to a variable degree, because only a fraction of vesicle content will hit the carbon surface (1).

For events from surround sites, τ_{rise} will be dominated by diffusion. Additionally, I_{peak} of similar vesicles is a decreasing function of the distance from the release site to the electrode surface (1,2). It can thus be expected that for surround sites on average I_{peak} decreases as a function of τ_{rise}. Therefore, I_{peak} was plotted as a function of τ_{rise} for individual cells (Fig. S1B) as well as for pooled data derived from several cells (not shown). As expected, I_{peak} decreased significantly with τ_{rise} increasing in the range from 0.2 to 15 ms. By excluding events with $\tau_{rise} > 3$ ms (10-30% of detected events), I_{peak} is no longer related to τ_{rise}. Examination of 17 PC12 cells yielded similar results. The mean τ_{rise} amounted to 0.89 ± 0.03 ms (*N*=365 events), 70% of these events have $\tau_{rise} \leq 1$ms and the median value of τ_{rise} amounted to 0.59 ms. Therefore, throughout this study the criterion $\tau_{rise} < 3$ ms is used to accept events from "near" release sites only.

Templates for event detection are slid along the traces and optimally scaled to fit the event. The two separate templates to detect spikes and "stand-alone-foot" events (SAFs) were created from recorded data by averaging ~10 manually detected events. The template-matching threshold was set at 3, i.e., detection of events with amplitudes of at least 3 times the noise standard deviation (cf. 3). Event detection based on amplitude threshold-crossings (peak noise amplitude) gives comparable results (not shown). However, template detection was preferred as it automatically compensates for changes in background noise, contrary to threshold detection, and the same noise threshold setting can thus be used on all our data.

Exocytotic events fitted with exponential functions

The Gaussian mixture analysis classifies events in one of the three clusters and subsequently events were traced back in the amperometric recording. A function defined in Clampfit (pClamp 9) was fitted to the selected events. The fitting started at the moment of fusion pore dilation, i.e., at the moment where baseline current, or prespike foot current if present, crosses the dI/dt of the rising phase of the exocytotic event.

1. S- and L-spikes were fitted according to:

$$I(t) = I_o \cdot \left\{ (1 - e^{-t/\tau_{rise}}) \cdot e^{-t/\tau_{decay}} \right\} \qquad [1]$$

where I_o is the instantaneous current (see also text and figure 1B for details). τ_{rise} and τ_{decay} are respectively the time constants of the rise and decay phases and are free parameters. This description was used to estimate release parameters and should be regarded as an approximation neglecting the sigmoidal beginning of the events and deviations of their mono-exponential decay. Extrapolation of the (fast) exponential decay to the start of the fusion pore dilation yielded I_o.

2. SAF-events could not be described by eq. [1] and were fitted to:

$$I(t) = I_o \cdot \left\{ (1 - e^{-t/\tau_{rise}}) - (1 - e^{-(t - \Delta t)/\tau_{decay}}) \cdot F(t > \Delta t) \right\} \qquad [2]$$

where I_o, τ_{rise} and τ_{decay} are defined as above and F(t) is the following logistic function:

$$F(t) = \frac{-1}{1 + \left(\frac{t}{\Delta t} \right)^{20}} + 1 \qquad [3]$$

The exponent to which $(t/\Delta t)$ is raised, determines the speed of the transition between the steady state phase and the decay phase. Since the underlying process is unknown (e.g. collapse of a catecholamine (CA) depot in the dense core or delay of fusion pore closure), we tentatively took the exponent equal to 20, in order to have a transition lasting a few ms (time constant about 3 ms). This model yielded a good fit with the experimental data.

Supplementary Results

Two-dimensional Gaussian mixture analysis for spikes

Scatter plots of log Q vs. log I_{peak} (Fig. S2A), log I_{peak} vs. log τ_{decay} (Fig. S2B) and log Q vs. log t_{50} (Fig. S2C) were fitted with mixtures of two-dimensional Gaussian functions. Two Gaussian functions were necessary to adequately fit the above mentioned relations between the spike parameters, clearly indicating the presence of two separate clusters of spikes denoted by L and S. Clusters identified in PC12 cells are remarkable similar compared to chromaffin cells. Each fitted cluster is assigned a Gaussian with its median in the center of the cluster and with a standard deviation that measures the spread of the cluster. The centers of the clusters are given in table S1. Notably, the centers obtained from the two-dimensional mixture analysis correspond well (less than a factor of 2) with the median values from the one-dimensional distributions of these spike parameters (Fig. 2).

Plotting log Q as a function of log I_{peak} indicates that Q and I_{peak} are directly proportional for both S- and L-events (Fig. S2A). For both PC12 and chromaffin cells, median Q as well as median I_{peak} of L-spikes are significantly ($p < 0.0001$) larger than those of S-spikes. Notably, the small S-spikes of both PC12 and chromaffin cells have comparable median peak amplitudes.

When log I_{peak} is plotted as a function of log τ_{decay} an elongated L-cluster and an almost spherical S-cluster are identified (Fig. S2B). L-events are approximately inversely proportional to τ_{decay}; a large L-spike will thus decay faster than a smaller L-spike. On the contrary, for the S-events I_{peak} and τ_{decay} are hardly correlated. In both cell types, L-spikes have a significantly larger median I_{peak} and smaller τ_{decay} compared to S-spikes ($p < 0.0001$).

The relation between log Q and log t_{50} is plotted in Fig. S2C, revealing an almost spherical L-cluster and an elongated S-cluster. For L-events, log Q and log t_{50} are hardly correlated, indicating that quantal size and the half-width are not or only weakly related. On the contrary, the data points of the S-cluster are moderately correlated and the slope of the regression line close to 1. This means that the quantal size of these spikes is approximately proportional to the half-width of the event. In PC12 and chromaffin cells, the median quantal size of L-spikes is significantly larger than of S-spikes ($p < 0.0001$), though the median t_{50}s of these spikes are very comparable (Table S1).

The center values of I_{peak} of the L- and S-cluster found in the log Q-log I_{peak} scatter plots (Fig. S2A) correspond well with the centers obtained from the clusters found in the log I_{peak}-log τ_{decay} plot (Fig. S2B). Similarly, the center values of Q of the L- and S-spikes found in the log Q-log I_{peak} scatter plots (Fig. S2A) correspond very well with the centers obtained from the clusters found in the log Q-log t_{50} plot (Fig. S2C). This indicates that from fitting the log Q-log I_{peak}, I_{peak}-log τ_{decay} or log Q-log t_{50} the same clusters of L- and S-events are identified, strongly supporting the view that a distinct population of L-events (large Q and I_{peak}, small τ_{decay}) coexists with a distinct population of S-events (small Q and I_{peak}, large τ_{decay}). These spike populations not only differ in Q, I_{peak} and decay kinetics, but also in their relation between I_{peak} and τ_{decay} as well as between Q and t_{50}. As discussed in the main article, this likely reflects different modes of exocytosis.

Two-dimensional Gaussian analysis for SAFs

The above described analysis is also applied to similar relations between the parameters of SAFs (Fig. S3), illustrating the similarities and differences between SAFs and spikes. SAFs are best fitted with a single two-dimensional spherical Gaussian distribution. The centers of the clusters are given in table S1. From the relation between log Q and log I_{peak}, it follows that the quantal size of the SAFs is proportional to their peak amplitude for both PC12 and chromaffin cells (Fig. S3A). From the relation between log I_{peak} and log τ_{decay} it follows that the peak amplitude is not related to the decay time constant of the SAFs. Note the similarity in the shapes of the clusters for PC12 and chromaffin cells (Fig. S3B). The relation between log Q and log t_{50} is depicted in Fig. S3C. Note that the shape of the SAF cluster in PC12 and in chromaffin cells is similarly elongated and regression analysis indicates that the quantal size is proportional to the SAF-duration. Also note that the shape of these SAF clusters is similar to the shape of the S-spike clusters (Fig S2C).

References

1. Haller, M., C. Heinemann, R.H. Chow, R. Heidelberger, and E. Neher. 1998. Comparison of secretory responses as measured by membrane capacitance and by amperometry. *Biophys. J.* 74:2100-2113.
2. Schroeder, T.J., J.A. Jankowski, K.T. Kawagoe, and R.M. Wightman. 1992. Analysis of diffusional broadening of vesicular packets of catecholamines released from biological cells during exocytosis. *Anal. Chem.* 64:3077-3083.
3. Clements, J.D., and J.M. Bekkers. 1997. Detection of spontaneous synaptic events with an optimally scaled template. *Biophys. J.* 73:220-229.

Supplementary Tables

Table S1: Median values of S-, L- and SAF-events clustered based on two-dimensional Gaussian functions depicted in Figs. S3-S4 for A) Log Q-log I_{peak}; B) Log I_{peak}-log τ_{decay}; C) Log Q-log t_{50}. Values correspond to the median center values (mcv; left) and slopes (sl) and correlation coefficient (r; right) of the different event clusters in PC12 and chromaffin cells.

	S		**L**		**SAF**	
A) Log Q - log I_{peak}	mcv	sl / r	mcv	sl / r	mcv	sl / r
PC12	28.8fC-5.2pA	1 / 0.83	95.4fC-20.0pA	1 / 0.67	16.8fC-1.1pA	2.1 / 0.54
Chromaffin	55.9fC-6.4pA	1 / 0.82	367.2fC-41.3pA	1 / 0.62	51.1fC-1.1pA	1.7 / 0.30
B) Log I_{peak} - log τ_{decay}						
PC12	4.7pA-5.3ms	-0.54 / -0.2	17.7pA-3.2ms	-1.3 / -0.56	1.1pA-5.8ms	0.003 / -0.01
Chromaffin	5.3pA-9.2ms	-0.07 / -0.03	35.3pA-5.3ms	-1.3 / -0.44	1.1pA-24.2ms	-0.22 / -0.29
C) Log Q - log t_{50}						
PC12	25.6fC-2.9ms	1 / 0.52	87.7fC-3.0ms	spherical / <0.2	16.8fC-11.0ms	1.3 / 0.77
Chromaffin	46.3fC-5.4ms	1 / 0.63	304.8fC-5.6ms	spherical / <0.2	51.1fC-31.9ms	0.8 / 0.66

Table S2: AIC-values corresponding to fits with 1 or 2 Gaussian distributions of event parameters (log Q, log I_{peak}, log, log τ_{decay} and log t_{50}) of spikes and SAFs obtained from PC12 and chromaffin cells. Fitting with 3 Gaussians (not shown) resulted in over-fitting as evidenced by fitting of clusters within clusters. Over-fitting could also occur in the case of double-Gaussian fits of SAF parameters (indicated by n.d.). AIC-values were calculated as described in the Materials and Methods Section. The best model is indicated by the lowest AIC-value (provided in bold). Notably, all spike parameters are best fitted with the sum of 2 Gaussians, except for log t_{50} in PC12 cells, which appears single Gaussian. On the contrary, SAF parameters are best fitted with a single Gaussian, except for log Q in chromaffin cells, which is best fitted with a double Gaussian.

		Spikes		**SAFs**	
AIC-values for Figure 2	**Nr of fitted Gaussians**	**PC12**	**Chromaffin**	**PC12**	**Chromaffin**
Log Q	1	12	3	**201**	443
	2	**6**	**-1**	206	**426**
Log I_{peak}	1	286	315	**230**	**180**
	2	**240**	**280**	n.d.	n.d.
Log τ_{decay}	1	431	232	**428**	**427**
	2	**403**	**223**	n.d.	n.d.
Log t_{50}	1	**77**	13	**59**	**35**
	2	79	**3**	63	38

Table S3: AIC-values corresponding to fits with 1-3 Gaussian distributions for the scatter plots depicted in Figure 4 for the relations between event parameters log Q vs. log I_{peak}, log I_{peak} vs. log τ_{decay} and log Q vs. log t_{50} for PC12 and chromaffin cells (spikes and SAFs). Fitting with 4 Gaussians (not shown) resulted in over-fitting as evidenced by fitting of clusters within clusters. The best model is indicated by the lowest AIC-value (provided in bold). The best fit for these relations, depicted in Figure 4, was obtained with the sum of 3 Gaussians for both PC12 cells and chromaffin cells.

AIC-values for Figure 4	**Nr of fitted clusters**	**PC12**	**Chromaffin**
Log Q - log I_{peak}	1	554	1635
	2	203	1238
	3	**106**	**1084**
Log I_{peak} - log τ_{decay}	1	988	1747
	2	668	1598
	3	**619**	**1538**
Log Q - log t_{50}	1	815	1733
	2	486	1392
	3	**436**	**1303**

Legends of the Supplementary Figures

Figure S1: Schematic representation of the electrochemical recording of exocytotic events (A). The sylguard-isolated carbon electrode is placed in direct contact with the neuroendocrine cell. A number of vesicles are shown at "far", "surround" and "near" release sites. Only fusion events occurring at "near" release sites, characterized by a rapid rise time, are completely detected with minimal diffusional delay. B) The relation between I_{peak} and τ_{rise} is used to exclude events from surround sites (see 'event detection and selection' for details). Data points were obtained from a single representative PC12 cell. The dashed line represents the upper boundary of 3 ms. Linear regression on all log-transformed data points (N=225) showed a significant decrease of I_{peak} as function of τ_{rise} ($p < 0.001$). For events with $\tau_{rise} < 3$ ms (N=200) such a relation did not exist (p=0.13). Consequently, the excluded events (~11%) were considered to represent exocytosis from surround sites. In this representative cell, 74% of the accepted events has rise time constants < 1 ms and the median value of τ_{rise} (indicated by the arrow) amounts to 0.55 ms. Inset: example of accepted (upper trace; τ_{rise} of 0.46 ms. Arrow indicates the prespike foot) and excluded event (lower trace; τ_{rise} of 8.3 ms) on basis of τ_{rise}.

Figure S2: Two-dimensional Gaussian mixture analysis of the relations between spike parameters of PC12 (left) and chromaffin cells (right) for log Q and log I_{peak} (A), log I_{peak} and log τ_{decay} (B) and log Q and log t_{50} (C). The scatter plots contain the pooled data from 17 PC12 (544 events) and 18 chromaffin cells (560 events). Two two-dimensional Gaussian distributions, denoted by L and S, were fitted to the data, yielding the different cluster centers [center ordinate, center abscissa]. Closed lines represent the variance of the clusters. Correlation coefficients were calculated from the fit. Linear regression of the fitted clusters yields the slope of the cluster. For all scatter plots, best fit is obtained on basis of the lowest AIC ($AIC_{2\ Gausians} < AIC_{1\ Gaussian}$). See table S1 for median center values, slopes and correlation coefficient of the different clusters.

Figure S3: Two-dimensional Gaussian mixture analysis of the relations between SAF parameters of PC12 (left) and chromaffin cells (right) for log Q and log I_{peak} (A), log I_{peak} and log τ_{decay} (B) and log Q and log t_{50} (C). The scatter plots contain the pooled data from 17 PC12 (145 events) and 18 chromaffin cells (146 events). A single two-dimensional Gaussian distribution was best fitted to the data, yielding the cluster center [center ordinate, center abscissa]. Closed lines represent the variance of the clusters. Correlation coefficients were calculated from the fit. Linear regression of the fitted clusters yields the slope of the cluster. SAFs contribute ~20% of the total number of events. Note the difference in scaling of the y-axis compared to Fig. S2. See table S1 for median center values, slopes and correlation coefficient of the different clusters.

Figure S4: Scatter plots of log Q vs. log t_{50} of only the first (A) or last 10 (B) events pooled from 17 PC12 cells. Three two-dimensional Gaussian distributions were fitted to the data to reveal similar clusters (SAF-, S- and L-events) as observed in Figure 4. The median quantal size of the first 10 events (of 17 cells) amounts to 18, 26 and 99 fC for SAF-, S- and L-events. This is not only very comparable with the median quantal size of the last 10 events (19, 27 and 91 fC), but also with the median quantal size of all events (Fig. 4C; 16, 24 and 84 fC). Similarly, the median t_{50} of the first 10 events amounts to 11.8, 3.2 and 3.2 ms for SAF-, S- and L-events, respectively. This is very comparable with the median t_{50} of the last 10 events (12.0, 2.8 and 3.1 ms) as well as with the median t_{50} of all events (Fig. 4C; 11.4, 2.9 and 3.0 ms). These data thus clearly indicate that clustering is not due to changes in Q or t_{50} over time.

Figure S5: Example scatter plots of log Q vs. log t_{50} of two individual PC12 cells (left) and two individual chromaffin cells (right). These data clearly show that the clustering of events observed in pooled data (Fig. 4) is not due to pooling and that similar clusters can be distinguished in scatter plots derived from single cell data. Clusters were incomplete or even absent (see e.g., the lower left scatter plot of a PC12 cell that apparently completely lacks L-events) in some cells due to the relatively small number of events.

Figure S1

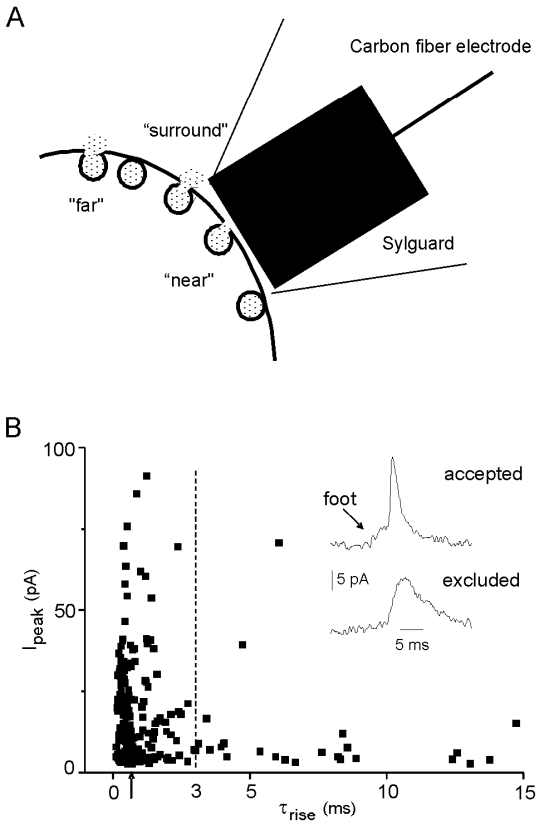

van Kempen et al.

Figure S2

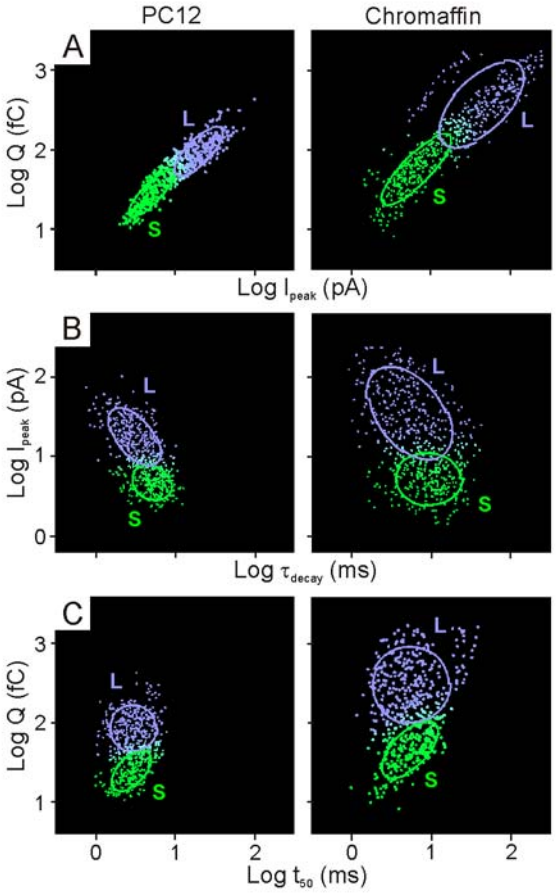

van Kempen et al.

Figure S3

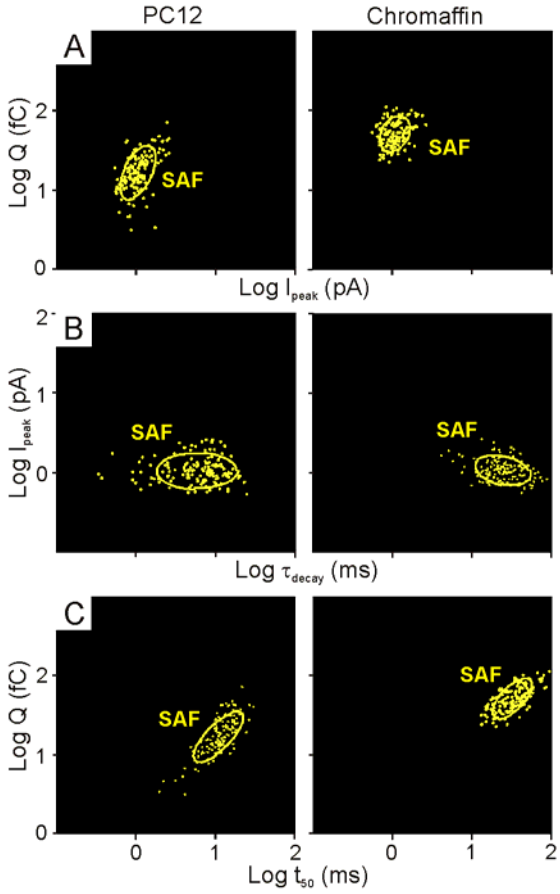

van Kempen et al.

Figure S4

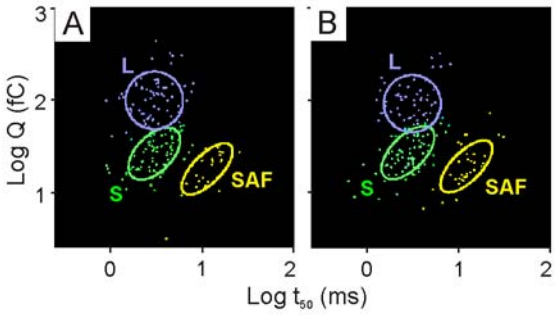

van Kempen et al.

Figure S5

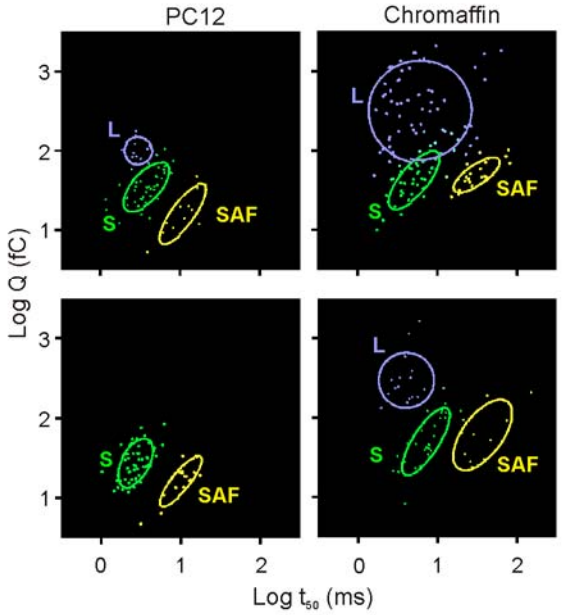

van Kempen et al.